1980-07

Theoretical Study of Finite-Amplitude Traveling Waves in Rigid-Walled Ducts: Behavior for Strengths Precluding Shock Formation

Coppens, Alan B.

Acoustical Society of America

Coppens, Alan B. "Theoretical Study of FiniteAmplitude Traveling Waves in RigidWalled Ducts: Behavior for Strengths Precluding Shock Formation." The Journal of the Acoustical Society of America 49.1B (1971): 306-318.
http://hdl.handle.net/10945/63147

Received 21 October 1969

Theoretical Study of Finite-Amplitude Traveling Waves in Rigid-Walled Ducts: Behavior for Strengths Precluding Shock Formation

ALAN B. COPPENS

U. S. Naval Postgraduate School, Monterey, California 93940

This paper presents three different solutions to a one-dimensional model of the propagation of finite-amplitude traveling waves in rigid-walled ducts. The first two solutions, in the nature of perturbation solutions, provide useful information for relatively weak waves; the distances for which the solutions are valid range from $\alpha_1 x \ll 1$ to $\alpha_1 x < \infty$, depending on the strength of the waveform and the particular solution considered. The third solution is based on a set of first-order coupled nonlinear differential equations with one independent and two dependent variables. This solution is useful for all values of $\alpha_1 x$ for strengths up to those necessary for shock formation. Results include graphs of relative harmonic distortion, predictions of waveform profiles, and representative graphs illustrating the dispersive behavior of the phase speeds of the individual harmonics.

INTRODUCTION

The topic of propagation of finite-amplitude traveling waves in rigid-walled ducts has received some attention in the literature,[1-3] but development of the subject has not been extensive, despite the facts that the propagation of sound in ducts is a frequently encountered situation and that plane-wave finite-amplitude studies in gases almost always require experimental configurations utilizing ducted propagation. The purpose of this paper is to present the results of three approaches to the problem, each of which is capable of describing the nonlinear behavior with reasonable simplicity for certain harmonics, values of distance from the source, and strength of the wave at the source. The present work is restricted to finite-amplitude effects that are not of sufficient strength to form a shock.

I. THE WAVE EQUATION

A one-dimensional nonlinear wave equation for propagation of acoustic waves in a duct with rigid walls has been established in a previous paper[4] and can be written as

$$\sum_{n=1}^{\infty} (\partial_x^2 - c_0^{-2}\partial_t^2 + D_n)u_n = \beta \partial_x \partial_t (\partial_x \xi)^2, \qquad (1a)$$

where

$$D_n \doteq -\delta_n \partial_x^2 + (\delta_n/n\omega)\partial_x^2 \partial_t, \qquad (1b)$$

$$\delta_n \doteq (G/S)(2n\omega)^{-\frac{1}{2}}[\nu^{\frac{1}{2}} + (\gamma-1)(\nu'/\gamma)^{\frac{1}{2}}] \text{ (Ref. 5)}, \qquad (1c)$$

$$\beta = 1 + \tfrac{1}{2}(B/A), \qquad (1d)$$

and where $u = \Sigma u_n = \partial_t \xi$ is the particle speed in the x direction, n is the harmonic number, c_0 is the phase speed in the limit $\beta = D_n = 0$, B/A (the parameter of nonlinearity) equals $\gamma - 1$ for a perfect gas, ω is the (angular) frequency of the first harmonic of the wave, γ is the ratio of specific heats of the fluid, ν is the kinematic viscosity, ν' is the thermometric conductivity, S is the cross-sectional area of the bore of the duct, and G is the perimeter of S.

This equation is valid under certain conditions:

(1) The boundary layer separating the mainstream of the fluid from the duct walls must have an effective thickness much smaller than the minimum transverse dimension of the cross-sectional area of the duct but large enough so that acoustic losses at the walls are the dominant dissipative effect.

(2) The surfaces of constant phase of the propagating signal must be planar across the tube except within the boundary layer.

(3) The thickness of the boundary layer must be much smaller than the wavelength of the highest acoustic frequency of interest.

(4) There must be no excitation of any transverse mode of the system, so that the amplitude of the wavefront is essentially constant outside the boundary layer.

(5) The gradient of the particle displacement, a measure of the Mach number, must be much less than unity. (This restriction allows the distinction between Eulerian and Lagrangian coordinates to be ignored.)

Terms containing the factor δ in Eq. 1 result from the formation of the boundary layer; energy dissipation in the mainstream has been assumed negligibly small.

While the formalisms to be developed are valid also for nonsinusoidal, but periodic, source excitations (within reasonable limits), we apply them herein only to sources moving sinusoidally. In all that follows, therefore, we assume a wave generated by a monofrequency source at $x=0$ and traveling in the $+x$ direction. The relevant boundary condition for Eq. 1 is thus

$$u(0,t)=U_0 \sin\omega t. \tag{2}$$

A. Linear Case

The solution of Eq. 1 for a traveling wave with the boundary condition of Eq. 2 in the limiting case of a linear process ($\beta=0$) can be seen to be

$$u/U_0=e^{-\alpha_1 x}\sin[\omega t-(k_0+\alpha_1)x], \tag{3a}$$

where

$$k_0=\omega/c_0 \tag{3b}$$

and

$$\alpha_1\doteq\tfrac{1}{2}k_0\delta_1. \tag{3c}$$

The effect of the wall losses is to introduce a *first-order* dispersion into the phase speed $c_1=\omega/(k_0+\alpha_1)$ such that

$$(c_1/c_0)^2=1-\delta_1. \tag{4}$$

The phase speed displays the interesting property of approaching the asymptotic value c_0 from below as the frequency ω increases. Thus, in a case where several frequencies are present, the waves of higher frequency will tend to propagate with higher phase speeds so that the traveling wave will show a continual spatial evolution as a result of the changing relative phases. This would suggest that, in the finite-amplitude region, steepening of the wavefront resulting from the constructive interference of the positive-going portions of the higher harmonics should tend to travel ahead of the positive going portion of the fundamental.

The attenuation resulting from wall losses depends on the square root of frequency. The Navier–Stokes attenuation expected from plane-wave propagation leads to losses that increase as the square of frequency. Thus, the dominant loss mechanism will shift from wall losses to Navier–Stokes losses above some transition frequency. In most experimental systems, this transition occurs at such high values of n as to be negligible in this discussion—it can be introduced easily, however, if desired.[4]

B. Nonlinear Case

In any treatment of the nonlinear case represented by Eq. 1, the fact that D has explicit frequency dependence not expressible as frequency raised to an integer power *requires* that the left-hand side of Eq. 1a be expressed as a sum over all frequencies present. This frequency dependence, along with that of the phase speed associated with each harmonic, excludes approaches based on the method of characteristics. We consider, therefore, methods based upon perturbation expansions or Fourier decomposition. Both of these techniques have proven successful in nonlinear studies of the Navier–Stokes equation[6,7] and, in that case, it has been shown that they are closely related, being different facets of solutions to Burger's equation.[8]

Certain descriptive parameters are common to these methods. We define here analogous quantities for use in what follows:

(a) The quantity

$$\frac{M\beta}{\delta_1}=\frac{\tfrac{1}{2}M\beta}{(\alpha_1/k_0)}, \tag{5a}$$

where

$$M=U_0/c_0 \tag{5b}$$

is the peak Mach number of the source, measures the ratio of waveform strength ($M\beta$) to fractional loss per wavelength (α_1/k_0), and is referred to as the *strength parameter*.

(b) Dissipationless theory[9] predicts a "discontinuity distance"

$$x_s=(M\beta k_0)^{-1}. \tag{6}$$

In terms of the dimensionless distance

$$l=\alpha_1 x, \tag{7}$$

this becomes

$$l_s=(2M\beta/\delta_1)^{-1}, \tag{8}$$

which expresses the (dimensionless) distance before which no shock would be expected to occur.

For sufficiently weak strength parameter, of course, no shock can ever form. When $M\beta/\delta_1$ is of sufficient magnitude so that a shock can result, it will be expected to form at distances larger than l_s.

II. SOLUTIONS

A. Perturbation Methods

It is well known that expansion of the nonlinear wave equation in Mach number results in a set of iterative, forced differential equations that admit sums of monofrequency components, each with spatially dependent amplitude, as solutions.

The perturbation expansion is written in the form

$$\frac{u}{U_0}=\sum_{m=1}^{\infty}\left(\frac{M\beta}{\delta_1}\right)^{m-1}v^{(m)}. \tag{9a}$$

TABLE I. Comparison of initial phase speeds for the nth harmonic between the linear prediction and the nonlinear prediction in the immediate vicinity of the source.

n	$\frac{[1-(c_n/c_0)^2]}{\delta_1}$ linear	nonlinear ($l \ll 1$)
1	1.00	1.00
2	0.71	0.85
3	0.58	0.79
4	0.50	0.76

The v's play the role of "normalized" dimensionless particle speeds and are convenient in characterizing the results of a perturbation approach. (They are of limited utility beyond the region of usefulness of the perturbation series, as is seen in later sections.) Examination of Eq. 1 (or any of the literature dealing with perturbation expansions of the nonlinear acoustic-wave equation) reveals that each $v^{(m)}$ is a sum over the contributions to this mth order term from several harmonics:

$$v^{(m)}=\sum_{j=0}^{[m/2]} v_{m-2j}{}^{(m)}, \tag{9b}$$

where the upper limit is the largest integer less than $m/2$. The numerical value of the subscript is the number of the harmonic. We henceforth write $n=m-2j$ and sum over n consistent with Eq. 9b. The term $v_n{}^{(m)}$ is of frequency $n\omega$, and the sum over n includes either all even or all odd harmonics equal to or less than the order number m. Recognizing that terms in b or δ in Eq. 1 are relatively small, we substitute temporal for spatial operators

$$c_0\partial_x=-\partial_t \tag{10a}$$

and

$$c_0{}^2\partial_x{}^2=\partial_t{}^2 \tag{10b}$$

into these terms. The result of these manipulations and substitution of Eq. 9 into Eq. 1 is the set of equations

$$\sum_n [c_0{}^2\partial_x{}^2-(1+\delta_n)\partial_t{}^2+(\delta_n/n\omega)\partial_t{}^3]v_n{}^{(m)}=\Phi^{(m)}; \tag{11a}$$

$$\Phi^{(m)}=-\delta_1\partial_t{}^2\sum_{i=1}^{m-1} v^{(i)}v^{(m-i)}, \quad m>1,$$

$$=0, \qquad m=1. \tag{11b}$$

1. Harmonic Power Series in l and $M\beta/\delta_1$

For values of l less than unity, it is plausible to assume for each term in Eq. 9 the form

$$v_n{}^{(m)}=A_n{}^{(m)}l^{m-1}\sum_{j=0}^{\infty}(-1)^j a_{nj}{}^{(m)}l^j \times\sin(n\omega\tau-R_n{}^{(m)}l), \tag{12a}$$

where τ is the "delayed time"

$$\tau=t-x/c_0. \tag{12b}$$

Substitution into Eq. 11 verifies that this form is acceptable for $j\leq 3$. Solutions must be generated in order of increasing m by successively calculating the forcing function for the next order from all solutions of lower order according to Eq. 11b, substituting this into the right-hand side of Eq. 11a, and solving for the required constants in Eq. 12. The results for the first four orders are

$$\begin{aligned}
v^{(1)}&=v_1{}^{(1)}=(1-l+0.50l^2-0.17l^3)\sin(\omega\tau-l),\\
v^{(2)}&=v_2{}^{(2)}=l(1-1.71l+1.46l^2-0.83l^3)\\
&\quad\times\sin(2\omega\tau-1.71l),\\
v^{(3)}&=v_3{}^{(3)}+v_1{}^{(3)}=\tfrac{3}{2}l^2(1-2.38l+2.84l^2-2.25l^3)\\
&\quad\times\sin(3\omega\tau-2.38l)-\tfrac{1}{2}l^2(1-2.14l\\
&\quad+2.36l^2-1.79l^3)\sin(\omega\tau-0.80l),\\
v^{(4)}&=v_4{}^{(4)}+v_2{}^{(4)}=(8/3)l^3(1-3.04l+4.63l^2-4.68l^3)\\
&\quad\times\sin(4\omega\tau-3.04l)-\tfrac{4}{3}l^3(1-2.84l\\
&\quad+4.12l^2-4.05l^3)\sin(2\omega\tau-1.47l).
\end{aligned} \tag{13}$$

Terms beyond $j=3$ depend upon powers in l beyond the first in the phase of the sine, and therefore cannot accurately be accounted for by Eq. 12a with $R_n{}^{(m)}$a constant.

Examination of the manipulations culminating in Eq. 13 reveals the following information:

(a) The leading term in the expansion for each $v_n{}^{(m)}$ is identical with that found from the Fubini-Ghiron[9] or Keck-Beyer[7] solutions for dissipationless nonlinear propagation; this is to be expected since the *initial* growth of the higher harmonics should be independent of either absorption or dispersion.

(b) The second term in each $v_n{}^{(m)}$ depends on the coefficient of the first term and on the attenuation constant for that harmonic (as observed in the linear limit) $\alpha_n=n^{\frac{1}{2}}\alpha_1$.

(c) Higher terms in each $v_n{}^{(m)}$ depend on all lower terms and on the dispersion in the phase speed.

(d) The observed phase speed for each harmonic in the limit $l\to 0$ is seen from Table I to be less than the value predicted in the linear limit by Eq. 4, but nevertheless to be of increasing value as a function of frequency, as suggested in the discussion following Eq. 4.

Calculation of the effective *total* attenuation constant from $2\alpha_{\text{eff}}I=-dI/dx$, where I is the total acoustic intensity, yields

$$\begin{aligned}\alpha_{\text{eff}}/\alpha_1&=1+2.15(M\beta/\delta_1)^2l^2\\&=1+0.54(x/x_s)^2\end{aligned} \tag{14a}$$

for small l. This ratio is somewhat smaller than that predicted for the Navier-Stokes case,[7]

$$\alpha_{\text{eff}}/\alpha_1=1+\tfrac{3}{4}(x/x_s)^2, \tag{14b}$$

and reflects the fact that we have $\alpha_n=n^{\frac{1}{2}}\alpha_1$ (duct case) rather than $\alpha_n=n^2\alpha_1$ (Navier-Stokes case), so that for

the same distortion and α_1 comparatively less energy is dissipated in the higher harmonics.

As can be seen from Eq. 13, convergence appears to be poor for larger l. Each series in l is alternating, which suggests that the calculated amplitude becomes undependable as soon as the last term becomes significant. Thus, $v^{(1)}$ should be accurate to within about 10% for $l<0.8$, whereas $v^{(4)}$ should be similarly accurate for $l<0.3$. Plots of $|v_n^{(n)}|$ are shown by the dashed lines in Fig. 1.

If we require contributions to lower harmonics from higher-order terms to be less than 10%, we have the approximate restrictions $(M\beta/\delta_1)l<0.5$ for the first harmonic and $(M\beta/\delta_1)l<0.4$ for the second harmonic. The conditions probably are increasingly stringent for the third and fourth harmonics. Thus, the solution appears useful for the lowest few harmonics up to distances such that either l/l_s is about 0.5 or l is about 0.3, whichever is smaller.

2. *Perturbation Expansion in* $M\beta/\delta_1$

If, instead of the assumption of Eq. 12a, we assume that a term

$$\Phi_{nj}^{(m)}=-\delta_1\partial_t^2F_je^{-E_jl}\cos(n\omega\tau-P_jl+\varphi_j) \quad (15)$$

appears on the right-hand side of Eq. 7a, then there will be an associated particular solution

$$v_{nj}^{(m)}=A_je^{-E_jl}\sin(n\omega\tau-P_jl+\varphi_j-\psi_j), \quad (16a)$$

where direct substitution reveals

$$\psi_j=\arctan[(P_j-n^1)/(E_j-n^1)] \quad (16b)$$

and

$$A_j=[nF_j/(P_j-n^1)]\sin\psi_j. \quad (16c)$$

This must be done for each component of frequency $n\omega$ in the forcing function. The sum over j of the resultant v_{nj}'s represents the total particular solution to the nth frequency component of the forcing function $\Phi^{(m)}$. The associated homogeneous solution

$$v_{nH}^{(m)}=A_{nH}^{(m)}e^{-n^1l}\sin[n\omega\tau-n'l-\theta_{nH}^{(m)}] \quad (16d)$$

is chosen so that the sum of homogeneous and particular solutions satisfies the boundary condition

$$v_n^{(m)}(0,t)=\sin\omega t, \quad n=m=1,$$
$$=0, \quad \text{otherwise}, \quad (2')$$

which ensures that the motion of the piston at $x=0$ is given by Eq. 2. The complete solution for the nth frequency component of the mth-order perturbation is, therefore,

$$v_n^{(m)}=v_{nH}^{(m)}+\Sigma_jv_{nj}^{(m)}, \quad (17)$$

where the sum on j extends over the number of separate terms in $\Phi_n^{(m)}$.

The first-order solution $v^{(1)}=v_1^{(1)}$ is the classical prediction given by Eq. 3. All homogeneous solutions will be of this form, with absorption and dispersion as predicted by the linearized wave equation.

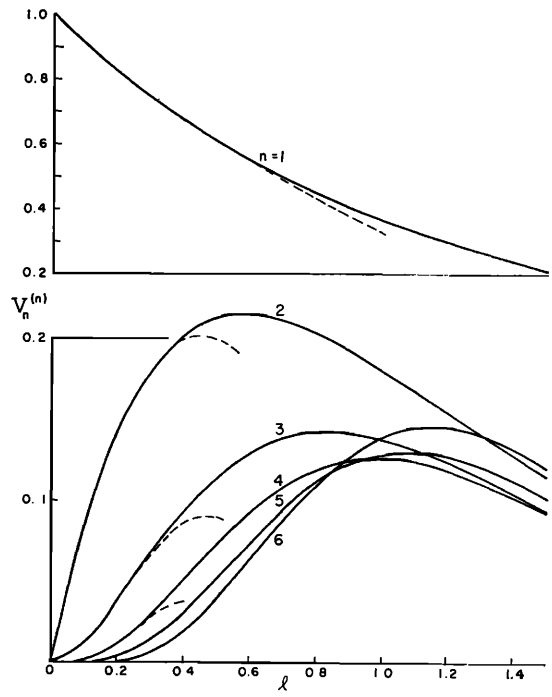

FIG. 1. Leading terms of the normalized dimensionless particle speeds associated with each of the first six harmonics of the propagating waveform as functions of the dimensionless distance $l=\alpha_1x$. – – –: results from the power series in l. ——: results from the second perturbation solution.

The second-order solution $v^{(2)}=v_2^{(2)}$ has the form

$$2(\sqrt{2}-1)v^{(2)}=e^{-\sqrt{2}l}\sin(2\omega\tau-\sqrt{2}l-\pi/4)$$
$$-e^{-2l}\sin(2\omega\tau-2l-\pi/4). \quad (18)$$

There are two terms, each with its own exponential decay and phase speed. The second of the two terms represents the particular solution resulting from the forcing term $\Phi^{(2)}$ and the first is the associated homogeneous solution. At small distances ($l\ll1$), the two terms are competitive and tend to interfere destructively; at large distances ($l\gg1$), the particular solution becomes negligibly small, leaving just the homogeneous term. Combination of terms in Eq. 18 to extract $|v^{(2)}|$ yields

$$(2-\sqrt{2})|v^{(2)}|=e^{-(1-1/\sqrt{2})l}\{\cosh[(2-\sqrt{2})l]$$
$$-\cos[(2-\sqrt{2})l]\}^{\frac{1}{2}}, \quad (19)$$

which is graphed in Fig. 1. This formula, an improvement over the prediction of Thuras *et al.*[1] since it includes the frequency dependence of the phase speed, is identical with a prediction of Blackstock as reported by Cruikshank[2] and with the second-order solution of Burns.[3]

The third-order solution, $v^{(3)}=v_3^{(3)}+v_1^{(3)}$, contains both third and first harmonics:

$$v_3^{(3)}=1.73e^{-3^1l}\sin(3\omega\tau-\sqrt{3}l-\pi/2)$$
$$+3.75e^{-2.41l}\sin(3\omega\tau-2.41l+\pi/2)$$
$$+2.02e^{-3l}\sin(3\omega\tau-3l-\pi/2)$$

TABLE II. Amplitudes and phases of the fourth-, fifth-, and sixth-order perturbation solutions (Eq. 17′) as functions of distance from the source.

l	$V_4^{(4)}$	$\Gamma_4^{(4)}$	$V_2^{(4)}$	$\Gamma_2^{(4)}$	$V_5^{(5)}$	$\Gamma_5^{(5)}$	$V_3^{(5)}$	$\Gamma_3^{(5)}$	$V_1^{(5)}$	$\Gamma_1^{(5)}$	$V_6^{(6)}$	$\Gamma_6^{(6)}$	$V_4^{(6)}$	$\Gamma_4^{(6)}$	$V_2^{(6)}$	$\Gamma_2^{(6)}$
0.1	0.002	−0.30	0.001	2.99	...	−0.36	...	2.93	...	...	...	...	...	...	...	...
0.2	0.012	−0.60	6	2.85	0.004	−0.73	0.003	2.72	...	−0.07	0.001	−0.86	0.001	2.61	...	−0.22
0.3	29	−0.90	0.015	2.70	0.014	−1.09	0.010	2.51	...	−0.13	7	−1.28	6	2.32	0.001	−0.34
0.4	51	−1.20	28	2.56	30	−1.45	21	2.30	0.001	−0.19	0.019	−1.70	0.017	2.05	2	−0.46
0.5	73	−1.49	41	2.41	51	−1.81	37	2.10	2	−0.25	38	−2.12	34	1.78	3	−0.57
0.6	93	−1.79	54	2.27	74	−2.16	54	1.89	2	−0.31	62	−2.53	56	1.52	6	−0.69
0.7	0.109	−2.07	65	2.12	94	−2.51	72	1.68	4	−0.37	87	−2.93	80	1.25	9	−0.81
0.8	120	−2.36	74	1.98	0.111	−2.85	87	1.48	5	−0.44	0.110	2.95	0.104	0.99	0.013	−0.94
0.9	126	−2.65	80	1.83	123	3.09	99	1.28	6	−0.51	128	2.55	125	0.73	16	−1.06
1.0	127	−2.93	84	1.69	129	2.75	0.108	1.08	7	−0.58	140	2.16	141	0.48	20	−1.18
1.1	125	3.07	85	1.54	131	2.42	113	0.87	8	−0.65	146	1.77	152	0.22	22	−1.30
1.2	120	2.79	85	1.40	128	2.08	115	0.67	8	−0.72	146	1.38	158	−0.03	25	−1.43
1.3	112	2.52	83	1.25	122	1.76	113	0.47	9	−0.79	141	1.00	158	−0.29	26	−1.56
1.4	103	2.25	80	1.11	113	1.43	110	0.28	9	−0.87	133	0.63	154	−0.54	27	−1.69
1.5	0.094	1.97	75	0.96	103	1.11	104	0.08	0.010	−0.94	121	0.26	147	−0.79	27	−1.82
1.6	84	1.71	71	0.82	0.092	0.79	0.097	−0.12	10	−1.02	109	−0.11	137	−1.03	27	−1.95
1.7	74	1.44	66	0.67	81	0.48	89	−0.32	10	−1.10	0.095	−0.47	125	−1.28	26	−2.08
1.8	65	1.18	60	0.53	71	0.17	81	−0.51	10	−1.18	82	−0.82	113	−1.52	25	−2.21
1.9	57	0.91	55	0.38	61	−0.14	73	−0.71	0.009	−1.26	70	−1.18	100	−1.76	24	−2.34
2.0	49	0.65	50	0.24	52	−0.45	65	−0.90	9	−1.34	59	−1.52	0.088	−2.00	23	−2.47
2.5	21	−0.61	28	−0.49	20	−1.91	33	−1.86	7	−1.76	21	3.10	41	3.10	14	−3.14
3.0	0.008	−1.81	15	−1.22	0.007	2.99	15	−2.81	5	−2.20	0.006	1.56	16	1.97	0.008	2.46
3.5	3	−2.95	0.008	−1.95	2	1.69	0.006	2.54	3	−2.66	2	0.13	0.006	0.87	4	1.76
4.0	1	2.24	4	−2.68	1	0.47	3	1.63	2	−3.13	...	−1.20	2	−0.19	2	1.06

and

$$v_1^{(3)} = -0.326e^{-l}\sin(\omega\tau - l + \pi/8) + 0.789e^{-2.41l}\sin(\omega\tau - 0.41l - \pi/8) - 0.604e^{-3l}\sin(\omega\tau - l - \pi/4). \quad (20)$$

The first term in each case, the homogeneous solution, is seen to be the most slowly decaying. (Decimal notation has been introduced where required for simplicity.)

As can be expected, the number of terms becomes progressively greater for higher orders: 15 terms for the fourth order, 57 for the fifth, 197 for the sixth. These higher-order solutions were obtained with the help of a digital computer, following much the same outline as given above.

Because of the great number of terms in these solutions and the fact that manipulation of the solutions in the form of Eq. 20 to obtain amplitude and phase becomes laborious, results for the fourth- through sixth-order solutions are written in the form

$$v_n^{(m)} = V_n^{(m)}\sin(n\omega\tau + \Gamma_n^{(m)}), \quad (17')$$

with amplitude and phase presented in numerical form in Table II.

At large distances, only the homogeneous contribution to each harmonic of each perturbation order remains significant (the higher attenuation constants reduce the other terms to negligibly small relative values). We can postulate, therefore, an asymptotic form through sixth order for the finite-amplitude traveling wave at large distances:

$$u/U_0 \to \sum_{m=1}^{6}\sum_{n}(M\beta/\delta_1)^{m-1}A_{nH}^{(m)}e^{-n^{\frac{1}{2}}l} \times \sin[n\omega\tau - n^{\frac{1}{2}}l - \theta_{nH}^{(m)}]. \quad (21)$$

Calculated values for $A_{nH}^{(m)}$ and $\theta_{nH}^{(m)}$ are presented in Table III. The increasing importance of correction terms as the harmonic and the order increase is apparent even in this region of large l.

TABLE III. Asymptotic values for amplitudes and phase angles in Eq. 21 through sixth order for the traveling wave in the region $l \gg 1$.

n	m	$A_{nH}^{(m)}$	$\theta_{nH}^{(m)}$ (rad)
0	1	1.00	0
	3	0.327	2.75
	5	0.098	−0.898
2	2	1.21	$\pi/4$
	4	1.00	−2.95
	6	0.551	−0.443
3	3	1.73	$\pi/2$
	5	2.42	−2.26
4	4	2.65	$3\pi/4$
	6	5.32	−1.54
5	5	4.18	π
6	6	6.69	$-3\pi/4$

Comparison of that part of the above solution through fourth order with the solution of Burns[3] shows that they are mathematically equivalent. Thus, this section demonstrates agreement with and extension of a previously known solution. We believe that this agreement gives strong evidence in support of the assertion that the relatively simple Eq. 1 is equivalent to the more complicated formalism of Burns (since both lead to the same results when solved by perturbation methods), at least within the limiting assumptions in Sec. I above.

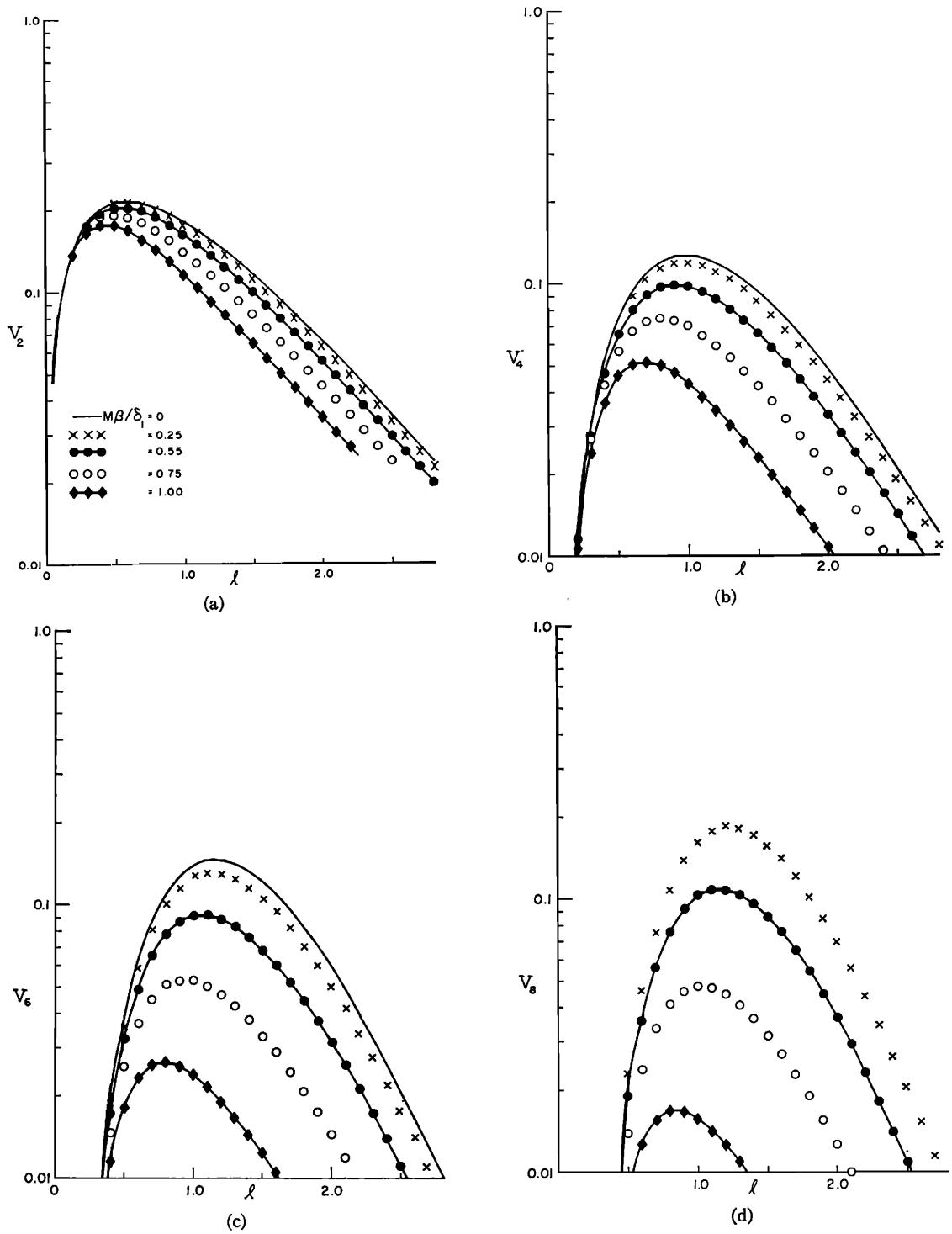

FIG. 2. Normalized dimensionless particle speeds for (a) the second, (b) the fourth, (c) the sixth, and (d) the eighth harmonic of the traveling wave as functions of the dimensionless distance l. Each harmonic is presented for various values of strength parameter as indicated by the legend in (a).

The amplitude $V_m^{(m)}$ of the *leading* term of each harmonic through the sixth is graphed in Fig. 1 for comparison with the results of Sec. II-A-1. The failure of the power-series representation of Sec. II-A-1 for all values of l except those in the immediate vicinity of the source is apparent.

There is little that is exceptional in the results of this section, except that correction terms to lower harmonics

from higher orders become increasingly important and, indeed, are *larger* than the leading terms for $M\beta/\delta_1>1$ and $l>1$ for the third and fourth harmonics. (These correction terms come from the fifth and sixth orders.)

While quantitative evaluation of the limits of accuracy of this sixth-order perturbation solution does not appear to be straightforward, some indicative constraints can be obtained.

Figure 2 displays the behavior of the even harmonics through the eighth as obtained by the results of Sec. II-B but presented in the form developed in this section. As can be seen, the amplitudes of the individual harmonics V_m show varying amounts of departure from the values predicted by the leading term in each harmonic series $V_m^{(m)}$; this leading term in each case is represented by the solid curve labeled $M\beta/\delta_1=0$. The difference in each graph between this curve and another for nonzero strength parameter is a measure of the importance of correction terms to the particular harmonic from higher perturbation orders. The correction terms become of increasing importance both at smaller distances and at smaller strength parameters as the number of the harmonic increases.

Since the series in each harmonic is quasialternating, it would appear that a conservative criterion to assure that the first through fourth harmonics of this sixth-order solution be within 10% of their true values for large l would be to require that $|u_4^{(6)}|/|u_4^{(4)}|<0.1$. This results in the limitation $M\beta/\delta_1<0.2$. This is consistent with examination of Fig. 2, which indicates that all harmonics below the sixth should be in close agreement with the leading term [that is, V_m is represented to within 90% by $V_m^{(m)}$ for $m<6$] for values $M\beta/\delta_1<0.25$. Notice, however, that the sixth harmonic fulfils this same criterion only for $l<1$.

As the strength parameter increases, higher harmonics become in poorer agreement at shorter distances. For example, if $M\beta/\delta_1=0.5$, then V_6 can be represented by $V_6^{(6)}$ within an error of 10% only for $l<0.4$, and higher strength parameters rapidly reduce the maximum useful l.

Thus, while the first four harmonics of the perturbation solution through sixth order appear adequately accurate for *all* l (and the sixth harmonic accurate for $l<1$) if $M\beta/\delta_1<0.25$, higher values of $M\beta/\delta_1$ restrict l quite drastically, especially for the higher harmonics, as can be inferred from examination of the curves for V_8 in Fig. 2. By way of comparison, Burns's criterion[3] of validity for his solution reduces to the requirement $l/l_s<0.5$, which is in reasonable agreement with the above discussion.

B. Computer Solution by Fourier Expansion

The two perturbation methods investigated above have provided reasonable predictive ability for rather limited values of distance and strength parameter. To extend these capabilities, we turn next to a formulation of Eq. 1 which is amenable to computer analysis. To begin, we integrate Eq. 1 with respect to time to obtain

$$\sum_{n=1}^{\infty}\left[\partial_x{}^2-c_0{}^{-2}\partial_t{}^2+\left(\frac{\delta_n}{n\omega}\right)\partial_x{}^2\partial_t-\delta_n\partial_x{}^2\right]\xi_n=\beta\partial_x(\partial_x\xi)^2. \tag{22}$$

Now, application of the judicious approximations

$$\partial_x{}^2\xi\doteq(c_0{}^{-1}\partial_t-\partial_x)(2c_0)^{-1}u, \tag{23a}$$

$$\partial_x{}^2\partial_t\xi\doteq(c_0{}^{-1}\partial_t-\partial_x)(2c_0)^{-1}\partial_t u, \tag{23b}$$

and

$$\partial_x(\partial_x\xi)^2\doteq-(c_0{}^{-1}\partial_t-\partial_x)(2c_0{}^2)^{-1}u^2 \tag{23c}$$

in those terms multiplied by either β or δ_n results in the appearance of the differential operator $(c_0{}^{-1}\partial_t-\partial_x)$ in all terms. This operator is removed by integration, and the time variable t is replaced by the delayed time τ. After these manipulations, Eq. 22 has the form

$$\sum_{n=1}^{\infty}\left[\partial_x+\tfrac{1}{2}\left(\frac{\delta_n}{c_0}\right)\partial_\tau-\tfrac{1}{2}(\delta_n/n\omega c_0)\partial_\tau{}^2\right]u_n=(\beta/c_0{}^2)u\partial_\tau u. \tag{24}$$

We now substitute into Eq. 24 for u the expression

$$u=\sum_{n=1}^{\infty}U_n(x)\sin[n\omega\tau+\phi_n(x)], \tag{25}$$

equate all terms of like frequency, define new dependent variables

$$\mathbf{s}_n=[U_n(x)/U_0]\sin\phi_n(x) \tag{26a}$$

and

$$\mathbf{c}_n=[U_n(x)/U_0]\cos\phi_n(x), \tag{26b}$$

and replace x with l. The results of these manipulations are two infinite sets of coupled nonlinear differential equations of first order in the single independent variable l:

$$\frac{d\mathbf{s}_n}{dl}+n^{\frac{1}{2}}(\mathbf{c}_n+\mathbf{s}_n)=\frac{n}{2l_s}\Big[\tfrac{1}{2}\sum_{j=1}^{n-1}(\mathbf{s}_{n-j}\mathbf{c}_j+\mathbf{c}_{n-j}\mathbf{s}_j)-\sum_{j=1}^{\infty}(\mathbf{s}_{n+j}\mathbf{c}_j-\mathbf{c}_{n+j}\mathbf{s}_j)\Big] \tag{27a}$$

and

$$\frac{d\mathbf{c}_n}{dl}+n^{\frac{1}{2}}(\mathbf{c}_n-\mathbf{s}_n)=\frac{n}{2l_s}\Big[\tfrac{1}{2}\sum_{j=1}^{n-1}(\mathbf{c}_{n-j}\mathbf{c}_j-\mathbf{s}_{n-j}\mathbf{s}_j)-\sum_{j=1}^{\infty}(\mathbf{c}_{n+j}\mathbf{c}_j+\mathbf{s}_{n+j}\mathbf{s}_j)\Big], \tag{27b}$$

where n ranges from unity to infinity. Were the mainstream absorption resulting from the viscous losses in the Navier–Stokes equation for plane waves to be included, then a term $+(n^2\alpha_{ns}/\alpha_1)\mathbf{s}_n$ would appear on the left-hand side of Eq. 27a and a term $+(n^2\alpha_{ns}/\alpha_1)\mathbf{c}_n$ in Eq. 27b. The quantity α_{ns} represents the plane-wave

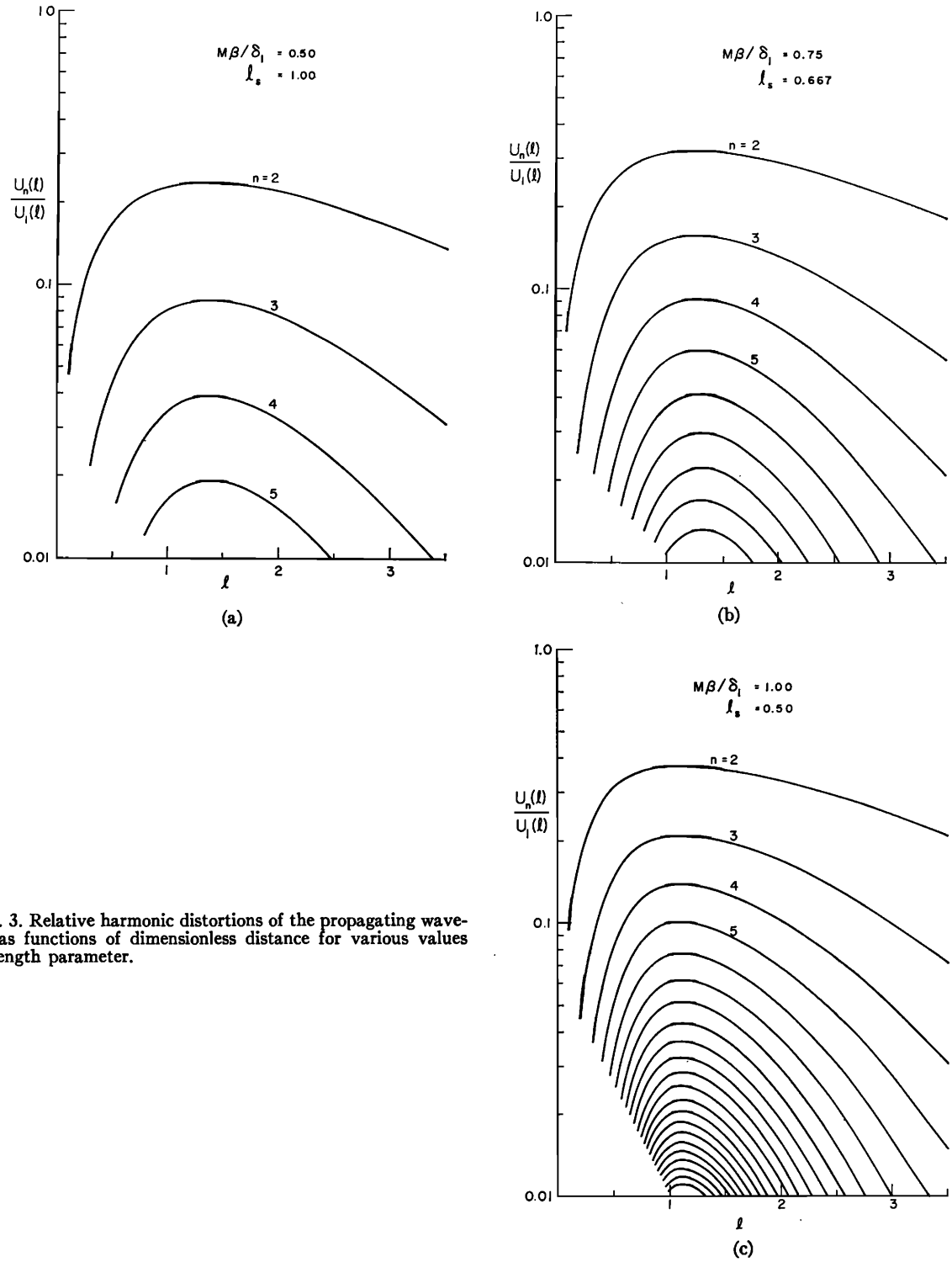

FIG. 3. Relative harmonic distortions of the propagating waveform as functions of dimensionless distance for various values of strength parameter.

(Navier–Stokes) absorption coefficient for the fundamental frequency. (The assumption here is that the loss mechanisms represented by α_{ns} and α_1 are noninteracting. This should be reasonable as long as both are small with respect to propagation constant.)

The decomposition of Eq. 1 into Eq. 27 has transformed the nonlinear wave equation into a simpler form amenable to a variety of computer-based techniques. All that is required is to specify the initial sets of U_n and ϕ_n at the face of the piston and then generate from

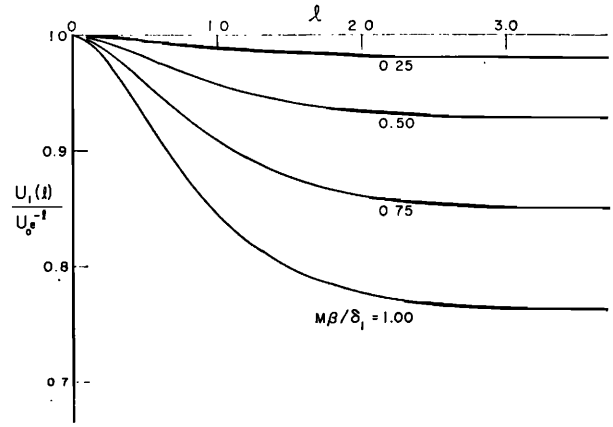

FIG. 4. Reduction in amplitude (beyond that of the linear case) of the fundamental harmonic of the propagating waveform as a function of dimensionless distance for various values of strength parameter.

the stipulated behavior of the source the resultant waveform at some finite distance by iterating over some suitably small increment Δ successively until the desired distance is reached. The essential restriction for straightforward application of Eq. 27 is that the infinite sums must be truncated, which places an upper limit on the strength parameter—harmonics above the highest one retained must be negligibly small.

We apply Eq. 27 to the case of the sinusoidally moving source, described by the boundary condition of Eq. 2, and employ a second-order Runge–Kutta iteration method[10] to obtain the spatial behavior of the distorting waveform:

(1) Values of the derivatives $\mathbf{s}_n'(l)$ and $\mathbf{c}_n'(l)$ are calculated for the distance l at which u is known by means of Eq. 27.

(2) Values of $\mathbf{s}_n(l+\Delta)$ and $\mathbf{c}_n(l+\Delta)$ are *estimated* at the new distance $l+\Delta$ by the formulas

$$\mathbf{s}_n(l+\Delta)=\mathbf{s}_n(l)+\mathbf{s}_n'(l)\Delta \tag{28a}$$

and

$$\mathbf{c}_n(l+\Delta)=\mathbf{c}_n(l)+\mathbf{c}_n'(l)\Delta. \tag{28b}$$

(3) Values for the derivatives $\mathbf{s}_n'(l+\Delta)$ and $\mathbf{c}_n'(l+\Delta)$ are obtained by substituting the results of step 2 into Eq. 27.

(4) Corrected values of $\mathbf{s}_n$ and $\mathbf{c}_n$ are calculated from

$$\mathbf{s}_n(l+\Delta)=\mathbf{s}_n(l)+\tfrac{1}{2}[\mathbf{s}_n'(l)+\mathbf{s}_n'(l+\Delta)]\Delta \tag{29}$$

and an identical formula in terms of $\mathbf{c}_n(l+\Delta)$. Errors in these values of $\mathbf{s}_n$ and $\mathbf{c}_n$ should be[10] of the order of Δ^3.

(5) This process is then repeated by evaluating derivatives at $l+\Delta$ according to step 1, etc.

For the cases treated herein, the initial set of U_n was obtained by calculating values at the distance $l=\Delta$ from dissipationless finite-amplitude theory; all ϕ_n were set equal to zero at this distance. The value of Δ was chosen as 0.001 or 0.002 for a program depending upon the time required to calculate the case in question. The maximum number of harmonics retained was 200. Any value of $(\mathbf{s}_n^2+\mathbf{c}_n^2)^{\frac{1}{2}}$ less than either 10^{-10} or 10^{-6}, again depending on time limitations, was discarded and that pair $(\mathbf{s}_n,\mathbf{c}_n)$ set equal to zero. At the worst, for all cases treated, errors in the values of the U_n were estimated to be less than or on the order of 3% until the magnitude of U_n fell below about 10^{-4} (the accuracy in each phase ϕ_n was similar to that in the associated U_n).

Calculations were performed for values of $M\beta/\delta_1$ less than or equal to unity. At the upper limit, those harmonics above the 150th began to display anomalous behavior, indicating that valid results could not be obtained for higher values of $M\beta/\delta_1$ without a substantial increase in the number of retained harmonics. Since the computation time was roughly proportional to the square of the number of retained harmonics, extension of this number was not feasible for the method of calculation used. The results for $M\beta/\delta_1=1.0$ appear to be accurate for all harmonics below at least the 100th since the deviations encountered in harmonics above the 150th show a sudden onset as functions of n: An abrupt change in the monatonic behavior of $U_n(x)$ and a sudden appearance of irregularities in $\phi_n(x)$, both as functions of n, occur in the region $0.9\lesssim l\lesssim 1.6$ for $n>150$, but all harmonic amplitudes and phases for $n<150$ are smooth functions of n consistent with those for smaller strength parameters. (As $M\beta/\delta_1$ is increased above unity, these deviations occur for lower n and a larger region of l and eventually lead to visible instabilities in the reconstructed profiles of the traveling waves.)

Curves showing the relative amplitudes of harmonics present to more than 1% in individual traveling waves are shown in Fig. 3. (Results for $M\beta/\delta_1=0.25$ were obtained but are not shown because only the first three harmonics had relative amplitudes greater than 1%.) All harmonics tended to peak together, so that there was an unambiguous region of l within which the waveform was maximally distorted. In all cases observed, this region shifted toward smaller l as the strength parameter increased but was always beyond the corresponding discontinuity distance.

As mentioned above, it was not possible to increase $M\beta/\delta_1$ until a shock formed owing to the limitation on the number of harmonics retained in the computer program. Extrapolation of the information in Fig. 3 to find a strength parameter for which U_n/U_0 approximated a $1/n$ dependence in the region of maximum distortion suggested that shock inception should occur for $M\beta/\delta_1$ somewhere between 1.25 and 1.50, but this cannot be confirmed without a more sophisticated treatment of Eq. 27.

Figure 4 presents the excess spatial decay of the fundamental for various values of strength parameter. For the range considered herein, it appears that nonlinear mechanisms of energy loss are strong in the region $l\lesssim 1.5$, but relatively weak for larger values of l.

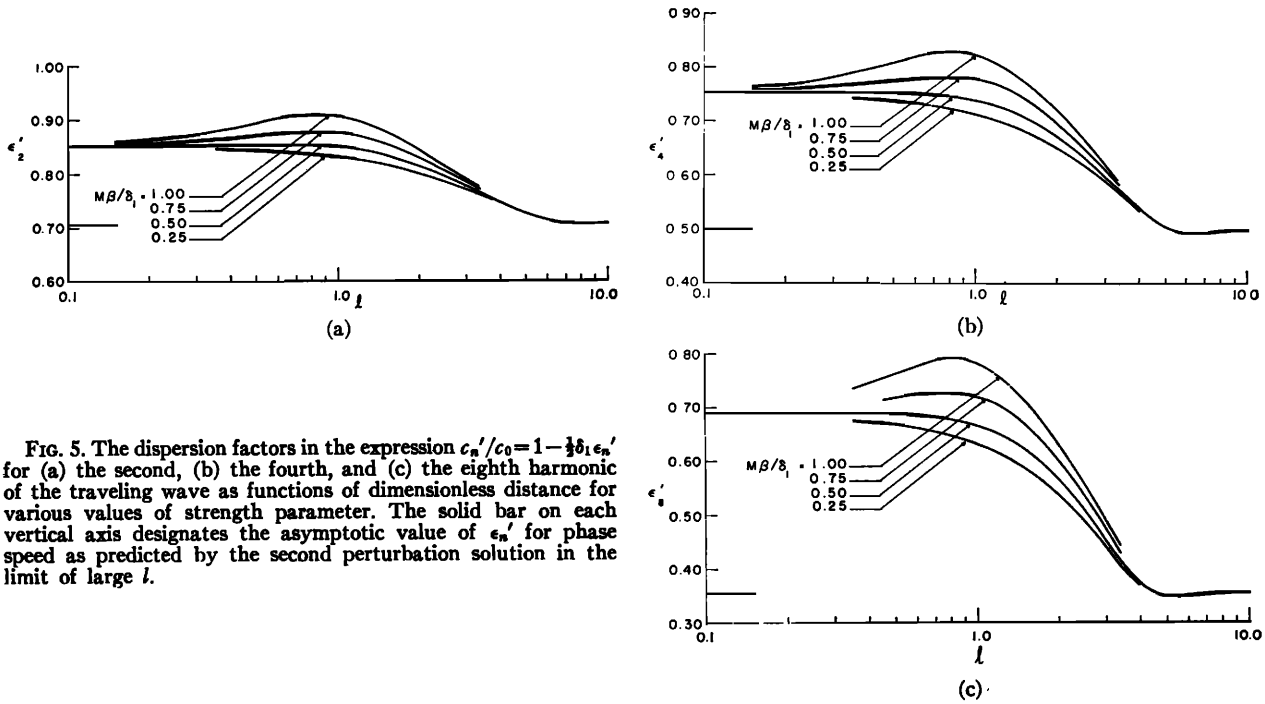

FIG. 5. The dispersion factors in the expression $c_n'/c_0=1-\frac{1}{2}\delta_1\epsilon_n'$ for (a) the second, (b) the fourth, and (c) the eighth harmonic of the traveling wave as functions of dimensionless distance for various values of strength parameter. The solid bar on each vertical axis designates the asymptotic value of ϵ_n' for phase speed as predicted by the second perturbation solution in the limit of large l.

The dispersive properties of the traveling waves were also investigated. Since the phase speed of a given harmonic depends on l, a distinction must be made between *average* phase speed c_n, defined by

$$u_n(x)=U_n(x)\sin[n\omega(t-x/c_n)], \tag{30}$$

which results in

$$\begin{aligned} c_n(l)/c_0&=x/(c_0t)=1+\tfrac{1}{2}\delta_1\phi_n/(nl)\\ &=1-\tfrac{1}{2}\delta_1\epsilon_n, \end{aligned} \tag{31}$$

and the *instantaneous* phase speed c_n' defined by

$$c_n'(l)=(\partial_t x)_{\text{CONSTANT PHASE, } n\text{th HARMONIC}}, \tag{32}$$

which results in

$$\begin{aligned} c_n'(l)/c_0&=1+\tfrac{1}{2}\delta_1(\partial_l\phi_n)/n\\ &=1-\tfrac{1}{2}\delta_1\epsilon_n'. \end{aligned} \tag{33}$$

The quantities ϵ_n and ϵ_n' have been introduced for convenience, since they are more sensitive measures of variations in dispersive effects than are the phase speeds. Manipulation reveals the relationships

$$c_n'=c_n+l\partial_l c_n \tag{34a}$$

and

$$\epsilon_n=\frac{1}{l}\int_0^l \epsilon_n' dl. \tag{34b}$$

Notice that in the linear limit $c_n=c_n'$ and $\epsilon_n=\epsilon_n'=n^{-\frac{1}{2}}$. Equation 34b reveals that ϵ_n' has stronger dependence on l than does ϵ_n, so that it seems more useful to examine the behavior of the instantaneous phase speed through ϵ_n'.

As an indication of the general behavior of c_n', we present ϵ_n' for the second, fourth, and eighth harmonics in Fig. 5. Computation revealed that ϵ_1' was somewhat in excess of unity in the region $l\sim 1.0$, but was never more than about 5% larger. Since a representative value for δ_1 is 0.01, this means that for $M\beta/\delta_1\leqslant 1.0$ the phase speed of the fundamental is essentially identical with that in the linear limit. The derivative $\partial_l\phi_n$ was estimated from the computer output over intervals of 0.1 in l so that ϵ_n' should be accurate to within a few percent. The behavior of phase speeds for $l\ll 1.0$ is in agreement with the predictions from the power-series perturbation solution. In the region of greatest distortion, the instantaneous phase speeds are *reduced* toward the value for the fundamental, the degree of reduction being greater for larger strength parameter. This is a surprising result, since one would expect that the tendency of higher harmonics to travel at higher phase speeds would lead to a general increase in phase speeds for lower harmonics in the region of greatest distortion, rather than the opposite effect. Nevertheless, these reductions in phase speeds are sufficiently weak to allow higher harmonics to lead the fundamental at all distances from the source. Notice that each instantaneous phase speed approaches the linear limit at large distance, as would be expected and as indicated by the asymptotic results for large l from the second perturbation solution. (The presence of the phase angles θ_{nH} in the asymptotic results apparently arises from the fluctuations in ϵ_n' for smaller l.)

Because of the large number of harmonics retained in the computer program, waveforms can be generated that should correspond to visual observations. The

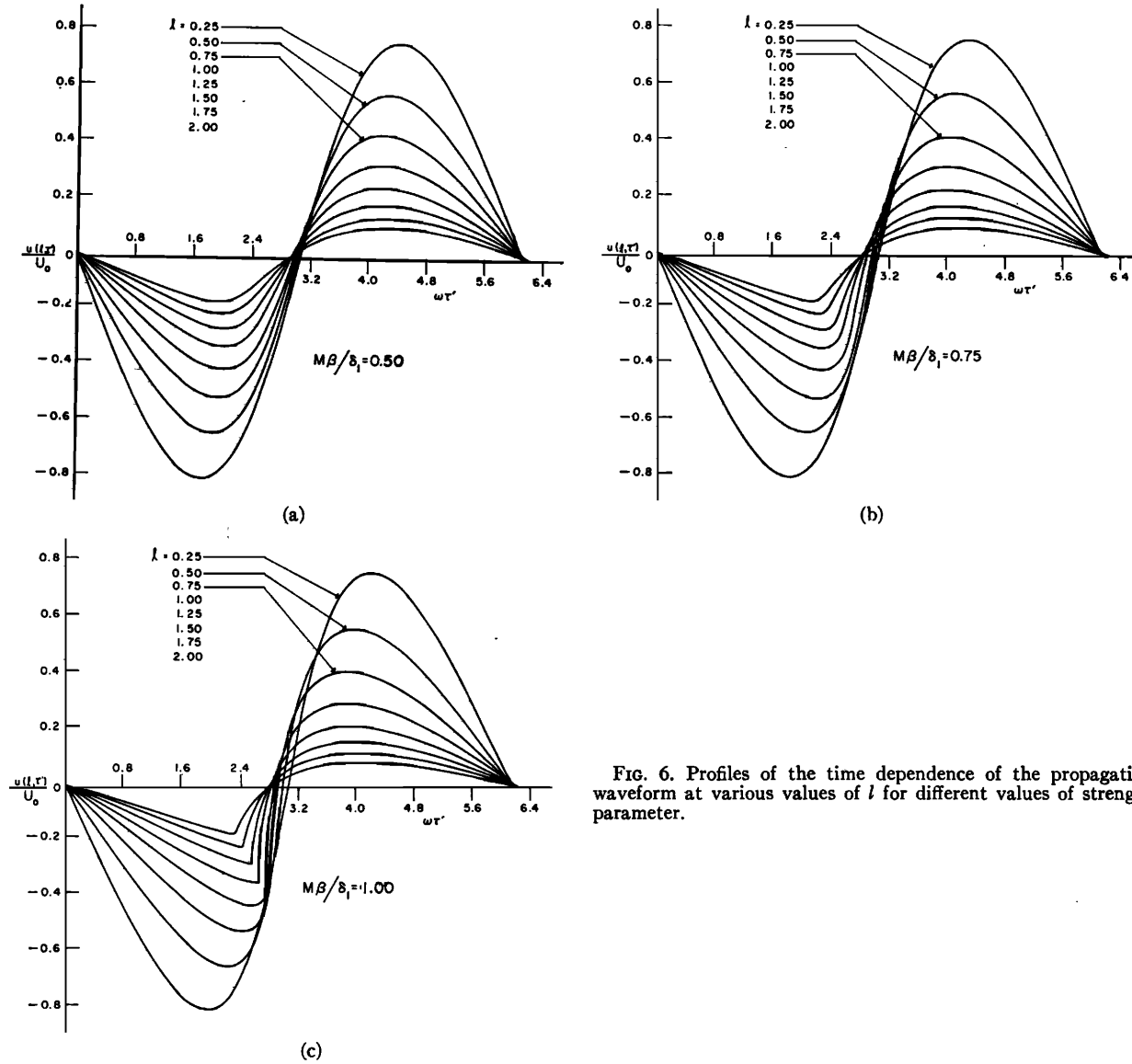

FIG. 6. Profiles of the time dependence of the propagating waveform at various values of l for different values of strength parameter.

limit on strength parameter used in these investigations assures that the absence of harmonics above the 200th will not noticeably affect the appearance of the waveforms. Graphs of the profiles of the traveling waves for values of l up to 2.00 are presented in Fig. 6. Results for $M\beta/\delta_1=0.25$ are not shown, because distortion was so weak that there was little visible departure from a sinusoid. For ease of comparison, the waveforms are presented as functions of $\omega\tau'$, where

$$\omega\tau'=\omega\tau+\phi_1(x)+\pi, \tag{35}$$

so that $\omega\tau'=0$ corresponds to the negative-going axis crossing of the first harmonic of Eq. 25. This allows the dispersive nature of the propagation to be readily apparent to the eye: Migration of the positive-going axis crossing of the waveform from $\omega\tau'=\pi$ to smaller values of $\omega\tau'$ as l increases is clear. Asymmetry of the waveform is evident, and the waveforms for $M\beta/\delta_1=1.0$ provide unmistakable evidence of the dispersive effects induced by the boundary layer. These profiles are in qualitative agreement with some experimental observations at higher strengths.[11]

Figure 6 and qualitative results for $M\beta/\delta_1>1.0$ strongly suggest that the shock to be found at higher strengths should lead the fundamental unambiguously and the propagating waveform should show clear departure from the sawtooth profile commonly encountered in weak shock waves traveling in nondispersive media.

III. THEORETICAL LIMITATIONS IN PRACTICE

The provisions of Sec. I required for the applicability of Eq. 1 can be investigated for representative experi-

mental configurations using air as the nonlinear medium.

The requirement that there be no excitation of cross modes in the duct can be fulfilled for all harmonics less than that leading to the lowest "sloshing" mode of the system. For this mode, the radial component of the function describing the acoustic pressure outside the boundary layer must behave as $J_1(nk_0r)$, subject to the boundary condition that the Bessel function reach its first maximum at the tube wall. This leads to the frequency requirement $n_{CM}2\pi fa/c_0 \sim 2$, where f is the fundamental frequency, n_{CM} the harmonic above which crossmodes can be excited, a the radius of the duct, and c_0 the speed of sound in air. This leads to the equation

$$n_{CM}=\lambda/(\pi a)=12\times10^3(fa)^{-1}, \tag{36}$$

where λ is the wavelength of the fundamental and all quantities are given in cgs units.

The restriction on the ratio of wavelength to boundary-layer thickness can be satisfied by stipulating that the acoustic wavelength of the n_λth harmonic be 10 times the boundary-layer thickness of the fundamental. (This should be a conservative criterion since boundary-layer thickness for monofrequency signals decreases with increasing frequency.) Since the boundary-layer thickness is given[5] by $2(2\nu/\omega)^{\frac{1}{2}}$, where ν is the kinematic viscosity, the lower limiting harmonic can be seen to be

$$n_\lambda=3\times10^4 f^{-\frac{1}{2}}. \tag{37}$$

The requirement that wall losses dominate mainstream losses can be estimated by finding the harmonic for which Navier–Stokes losses equal wall losses. Since the former grow as the square of the frequency and the latter as the square root, this harmonic designates the frequency limit above which bulk losses dominate. This harmonic, for air at standard conditions, is given approximately by

$$n_\alpha=3\times10^5/(fa^{\frac{1}{2}}). \tag{38}$$

This requirement can be relaxed if the Navier–Stokes losses are explicitly included in the left-hand side of Eq. 1, or if the additional terms are included in Eq. 27, in accordance with the discussion following that equation. With this emendation (which requires that these energy losses be additive and noninteractive), boundary-layer effects can be ignored for $n>n_\alpha$ because of the greater importance of bulk absorption. Dispersive effects would still remain, but should be small enough to allow the approximation $c_n=c_0$ for $n>n_\alpha$. Further, if $n_\alpha<n_\lambda$, then the requirement on the ratio of wavelength to boundary-layer thickness should become void because of the unimportance of the boundary-layer effects for $n>n_\alpha$.

Combination of Eqs. 36 and 38 results in the expression

$$n_\alpha/n_{CM}=25a^{-\frac{1}{2}}. \tag{39}$$

This formula indicates that the inequality $n_{CM}<n_\alpha$ is assured in any experimental system for which the duct radius is less than about 600 cm.

TABLE IV. Harmonics for which cross modes, bulk absorption, or boundary effects violate the assumptions required for the validity of Eq. 1.

f (Hz)	n_{CM}	n_α	n_λ
$a=3$ cm			
100	40	600	3000
1000	4	60	1000
$a=1$ cm			
100	120	3000	3000
1000	12	300	1000

Further manipulation of the above equations results in

$$n_\lambda/n_\alpha=f^{\frac{1}{2}}a^{\frac{1}{2}}/10 =a(120/n_{CM})^{\frac{1}{2}}. \tag{40}$$

The second line of the above equation reveals that n_λ may be expected to exceed n_α in magnitude if, for example, a is greater than 1 cm and n_{CM} less than about 100.

Table IV presents the values of n_{CM}, n_α, and n_λ to be expected for two different tube radii and two fundamental frequencies. These examples reveal that it is not difficult to ensure the inequalities $n_{CM}<n_\alpha<n_\lambda$ in a practical experimental system. Under these conditions, the remarks allowing extension of Eq. 1 to the inclusion of bulk absorptive effects are valid, so that Eqs. 1 and 27 can be modified as discussed above.

Thus, the essential difficulty in comparing experiment with theory lies with the influence of excited cross modes on the finite-amplitude waveform. There is little that can be said about this except that reasonable design of acoustic source and duct should ensure conditions minimizing the excitation of higher modes, and that study of the harmonic content and stability of the observed nonlinear waveform (over the cross-sectional area of the tube) can determine whether or not there is significant energy present in modes other than the plane-wave modes.

IV. CONCLUSIONS

Three forms of solutions to Eq. 1 have been developed:

(1) A power-series perturbation expansion provides simple expressions for the first four harmonics close to the source and for small values of the strength parameter. The solution is quite useful in the region $l<0.3$ and $l/l_s<0.5$ and directly provides information concerning amplitude and phase, which is extractable only with difficulty from the results of the second perturbation solution. (Indeed, rounding errors that can accumulate in numerical calculations of the second perturbation solution may result in large uncertainties in phase for $l<0.1$, where the various terms in each harmonic tend to be mutually cancelling.)

(2) A second perturbation solution, obtained for the first six orders, is useful but cumbersome for all l if the strength parameter is small. This solution offers extension beyond solution 1 above in that the restriction $l<0.3$ can be removed. The solution shows agreement with and extension of a solution obtained by Burns from a more complicated formalism. This suggests that the one-dimensional model represented by Eq. 1 contains implicitly the simplifying assumptions that had to be made explicitly by Burns to obtain tractable results. In contrast to the statement by Burns that fifth- and sixth-order perturbation solutions would extend the range of validity of this approach, it appears from the results of this investigation that the convergence properties of the higher-order solutions become increasingly poor, so that accurate predictive ability appears to be limited intrinsically by $l/l_s<0.5$ for this approach, regardless of the order to which the solution is taken. Additionally, the rapid increase in the number of particular solutions in the higher orders is prohibitive for analytical treatment of not only the higher harmonics but also the correction terms to lower harmonics from higher orders.

The requirement $l/l_s<0.5$ of both perturbation solutions, equivalent to $(M\beta/\delta_1)l<0.25$, can be interpreted as a limitation on the harmonic content of the distorted waveform within which the perturbation approach is valid. From Eq. 13, it can be seen that approximate limits of relative distortion are 25% second harmonic, 9% third harmonic, 4% fourth harmonic, etc. These low levels of distortion show that these solutions are useful only for weak finite-amplitude effects and can be expected to have little utility for any waveform possessing appreciable distortion.

(3) A computer-based iterative solution to the pair of coupled nonlinear first-order differential equations in Eq. 27 yields solutions valid for all distances and for values of strength parameter through unity. The computer results, while of necessity sacrificing some of the insights provided by the algebraic and trigonometric forms of the other approaches, allow a much larger region in l and $M\beta/\delta_1$ to be investigated and greatly increase the number of harmonics whose amplitudes and phase properties can be predicted. The numerical computations of instantaneous phase speeds demonstrate agreement with the first perturbation solution near the source and the second perturbation solution at large distances.

The validity of the loss term in Eq. 1 depends on acoustic wavelength being larger than boundary-layer thickness. This provides an explicit frequency limit beyond which Eq. 1 is not applicable without modification. While the theory of boundary-layer effects for acoustic processes wherein wavelength is not significantly larger than boundary-layer thickness does not appear to have been worked out, this restriction can be avoided if the experimental system is designed so that bulk absorptive effects dominate boundary-layer effects at a lower frequency. In that event, the inclusion of bulk effects can proceed as discussed above and the equations should then be valid for all harmonics.

The problem of the excitation of cross modes remains, however. There appears to be no way to forbid excitation of these modes, so that it can only be hoped that the particular system will be close enough to fulfilling the theoretically postulated boundary conditions to allow these modes to be excited only weakly. If a cross mode at a frequency corresponding to the nth harmonic is excited so weakly that it contains only a small fraction of the energy present in the plane-wave mode of this harmonic, it can then be expected that the perturbation resulting from this additional term will be small enough so that no major alterations of amplitudes and phases result. The theoretical model investigated herein should then be valuable at least as a reasonable approximation to the true physical situation.

Further work will be directed to the problem of extending the analysis of Eq. 27 in the hope of obtaining information for traveling waves strong enough to form shocks.

ACKNOWLEDGMENTS

The author should like to express his appreciation to D. E. Harrison for his suggestions and help with the formulation of the computer program, to J. V. Sanders for many useful conversations concerning practical aspects of this nonlinear problem, and to the computer facility of the Naval Postgraduate School, which made possible the analysis of Eq. 27.

[1] A. L. Thuras, R. T. Jenkins, and H. T. O'Neil, J. Acoust. Soc. Amer. **6**, 173–180 (1935).
[2] D. B. Cruikshank, J. Acoust. Soc. Amer. **40**, 731–733(L) (1966).
[3] S. H. Burns, J. Acoust. Soc. Amer. **41**, 1157–1169 (1967).
[4] A. B. Coppens and J. V. Sanders, J. Acoust. Soc. Amer. **43**, 516–529 (1968).
[5] D. E. Weston, Proc. Phys. Soc. (London) **B66**, 695–709 (1953).
[6] R. D. Fay, J. Acoust. Soc. Amer. **3**, 222–241 (1931).
[7] W. Keck and R. T. Beyer, Phys. Fluids **3**, 346–352 (1960).
[8] D. T. Blackstock, J. Acoust. Soc. Amer. **39**, 411–413(L) (1966).
[9] E. Fubini-Ghiron, Alta Frequenze **4**, 530–581 (1935).
[10] M. Abramowitz and I. A. Stegun, Eds., *Handbook of Mathematical Functions*, Nat. Bur. Stand. (U.S.) Appl. Math. Ser. 55 (U.S. Govt. Printing Office, Washington, D. C., 1965).
[11] J. L. McKittrick, D. T. Blackstock, and W. M. Wright, J. Acoust. Soc. Amer. **42**, 1153(A) (1967).